Multiparameter Mapping of Polymer Properties for Fast Thermolysis of Powder Moldings

J. H. SONG,[1] J. R. G. EVANS,[1] M. J. EDIRISINGHE,[1] E. H. TWIZELL[2]

[1] Department of Materials Engineering, Brunel University, Uxbridge, Middlesex UB8 3PH, United Kingdom

[2] Department of Mathematics and Statistics, Brunel University, Uxbridge, Middlesex UB8 3PH, United Kingdom

Received 17 November 1997; accepted 24 February 1998

ABSTRACT: Ceramic or metal injection molding involves the shaping of a crowded suspension of particles in a polymer that is later removed by thermolysis. During heating, degradation products dissolve in the parent polymer and diffuse to the free surfaces where evaporation occurs. If heated too rapidly in the initial stage, the solution at the center of the molding boils and a bubble forms. This article explores the implications of a multiparameter model that predicts the highest permissible heating rate in terms of polymer properties and maps the outcome. The aim is to develop criteria for the deliberate synthesis of thermally labile copolymers from a knowledge of the desirable property combinations. © 1998 John Wiley & Sons, Inc. J Appl Polym Sci 70: 545–557, 1998

Key words: diffusion; thermal degradation; mathematical modeling; ceramic processing

INTRODUCTION

In metal and ceramic injection molding, crowded suspensions containing 50–70 vol % of powder in a polymer vehicle are prepared by high shear mixing prior to forming. The vehicle, which has a transient role, is removed, usually by slow heating, before sintering the powder assembly that should retain its shape and be free from defects.[1–3] Every stage in this sequence depends on different properties of the polymer. The most difficult stage, particularly for large sections (>15 mm), is the removal of the vehicle by controlled thermolysis. Procedures have been established to use gravimetric control to determine the rate of heating[4] and to use composite thermogravimetry to select combinations of organic media to give a steady weight loss on heating,[5,6] but these approaches address only the rate at which volatile degradation products are evolved. They do not consider the mass transport kinetics in a large section molding.

Low molecular weight organic vehicles are lost by evaporation from the surface of moldings,[7] and the use of oxidative atmospheres introduces a surface reaction with shrinking core kinetics.[8] Often polymer degradation takes place in a nonoxidizing atmosphere.[1] Thermal degradation accompanies these processes and, when the temperature is above the ceiling temperature, takes place uniformly throughout the section liberating low molecular weight products of decomposition. These dissolve in the parent polymer, and evaporation from the surface produces a concentration profile that is the driving force for outward diffusion of products in solution in the continuous phase. If the temperature rises above the boiling point of the solution at the center of the section, where the low molecular weight component is most concentrated, boiling occurs and a defect is produced.

Correspondence to: J. R. G. Evans.

Contract grant sponsor: EPSRC; contract grant number: GR/H93545.

Journal of Applied Polymer Science, Vol. 70, 545–557 (1998)

 CCC 0021-8995/98/030545-13

This occurs in the critical stage when all pores are filled by organic vehicle. Later, as the polymer fraction reduces, continuous porosity forms and gas transport paths become available. The critical stage has been recognized and modeled for steady state[9] and unsteady state diffusion.[10] The model has been extended to consider the development of various porosity configurations,[11] for the principal geometries,[12] for gas transport in a porous outer layer,[13] and for a surrounding powder bed.[14] The model has been tested experimentally using coarse alumina powder and poly(α-methylstyrene) at atmospheric pressure[10,12] and at elevated pressures.[15] In these models, polymers that undergo thermal decomposition to monomer are considered because the existence of more than one degradation product complicates the analysis immensely. The diffusion coefficient for each product is affected by the concentration of every other product, and multicomponent interaction parameters would be needed in deducing the boiling points. Several polymers that decompose to monomer, such as the short ester group methacrylates, poly(α-methylstyrene), or polyoxymethylene can be used in ceramic processing.

An initial exploration of the implications of the model has been conducted to rank the influence of monomer and polymer properties.[16] This was achieved by holding a set of default parameters corresponding to poly(α-methylstyrene) and its monomer and varying each one individually over the range of values that is consistent with known polymers. This type of sensitivity analysis is restrictive in that it does not disclose heating rate maxima resulting from simultaneous variation in all parameters.

From this sensitivity[16] analysis, the parameters that have been found to influence the critical heating rate strongly fall into three groups: (1) those controlling diffusion coefficient as calculated from free volume theory,[17] namely pre-exponential coefficient D_0, activation energy for diffusion E_d; (2) those that control the shape of the thermogravimetric curve, namely specific rate constant K_0 and activation energy E; and (3) the parameters that influence the boiling point of the monomer, namely ΔH_{vap} and i the logarithm of the pre-exponential coefficient in the Clausius–Clapeyron relationship.

These parameters give a preliminary indication of how the synthesis of thermally labile polymers for ceramic processing might be approached. Thus, the size of the degradation product molecule and its polarity influence ΔH_{vap} and could be influenced by introducing weak links to control chain scission sites. The problem is that, while increasing the diffusant molecular size increases the boiling point it is likely to reduce D_0, another sensitive parameter; and so, a delicate balance of "design features" for the polymer emerge.

The aim of this article is to explore the effects of varying, in combination, the parameters that have been found to be influential. Data so generated, which are potentially vast, should be capable of being comprehended and interpreted on a physical basis. In the past, polymers selected for ceramic processing have tended to be available production grades. They have not been synthesized for their thermal lability; indeed, quite the reverse. There is scope for advances in polymer synthesis to be applied to ceramic processing, and this work is intended to pave the way for this.

THEORY

An infinite cylinder of radius r_0 containing an inert filter, such as a ceramic powder, at volume fraction V_c, is considered. A single polymer that saturates the pore space, which consequently has a volume fraction $1 - V_c$, is assumed to degrade exclusively to the monomer. The molding is heated at a constant heating rate, Z, that is sufficiently low for the temperature gradient caused by transient heat transfer to be neglected. This condition holds for the experimental validation of the model where the heating rates are low or where high uniform rates of heating can be achieved (e.g., microwave-assisted). The mathematical model determines the critical linear heating rate, Z_c, at which the peak vapor pressure along the axis of the cylinder is below the ambient pressure throughout the heating process. Thus, defects due to boiling of the monomer in solution in the parent polymer do not occur.

As the polymer degrades, it is considered to recede in the interparticle pore space[11] (Fig. 1). Assuming that the initial radius of the cylinder is r_0, the radius r_n, of the shrinking undegraded core at some subsequent time t_n, is given by

$$r_n = r_0 h^{1/2} \tag{1}$$

where h, the remainder weight fraction of polymer, is defined by

$$h = \exp\left\{ -\frac{K_0 R T^2 \exp(-E/RT)}{ZE} \times \left[1 - \frac{2RT}{E} + \frac{6R^2T^2}{E^2} \right] \right\} \tag{2}$$

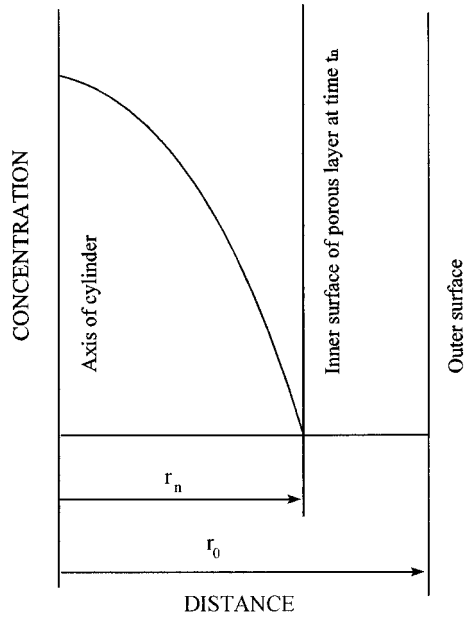

Figure 1 Schematic diagram of the shrinking undegraded core model for a cylinder with initial radius r_0.

(see, e.g., Evans and colleagues[10]). Descriptions of the symbols used in eq. (2) and throughout the article are given in the Nomenclature section.

The monomer concentration within the undegraded cylindrical core satisfies the partial differential equation

$$\frac{\partial C}{\partial t} = \frac{1}{r}\frac{\partial}{\partial r}\left(rD\frac{\partial C}{\partial r}\right) + \dot{Q};\ 0 < r < r_n;\ t > t_n \quad (3)$$

in which $\dot{Q}$, the rate of generation of monomer based on unit volume of suspension, is given by

$$\dot{Q} = \dot{q}\rho_p(1 - V_c) \quad (4)$$

where

$$\dot{q} = K_0 h\ \exp(-E/RT) \quad (5)$$

is the rate of production of monomer based on the mass of polymer. The diffusion coefficient, D, for monomer in the unfilled polymer, varies with temperature, T, and with concentration, C. The free volume theory of diffusion[17] can be used to define D over a wide range of values of T and C from the expression

$$D = D_{01}(1 - \phi)^2(1 - 2\chi\phi)\exp\{-[W_1V_1(0) + W_2\xi V_2(0)]/(V_f/\omega)\} \quad (6)$$

for diffusion in the continuous phase, where ϕ, the volume fraction of monomer in polymer, is given by

$$\phi = W_1V_1/(W_1V_1 + W_2V_2) \quad (7)$$

and the diffusion constant D_{01} is given by

$$D_{01} = D_0\ \exp(-E_D/RT) \quad (8)$$

The expression for V_f/ω is

$$V_f/\omega = (K_{11}/\omega)W_1[(c_2)_1 + T - (T_g)_1] + (K_{12}/\omega)W_2[(c_2)_2 + T - (T_g)_2] \quad (9)$$

and

$$\omega V_1(0)/K_{11} = 2.303(c_1)_1(c_2)_1, \quad (10)$$

$$\omega V_2(0)/K_{12} = 2.303(c_1)_2(c_2)_2. \quad (11)$$

Maxwell's equation[18] was used to find the effective diffusion coefficient in the composite, D_c, for the condition where the diffusion coefficient in the dispersed phase is zero.

$$\frac{D_c}{D} = 1 - \frac{3V_c}{V_c + 2} \quad (12)$$

The vapor pressure of the monomer at the outer surface is assumed to be zero because, at this surface, monomer is removed by a fast-flowing sweep of inert gas in the practical context. In previous work, the effect of transport through the porous outer layer has been taken into account;[13,19] but, if the particles are not ultrafine, this resistance is small compared with diffusion in the polymer-containing core and was neglected in the present work.

The concentration of monomer at the center is calculated at each time increment on the linear rate of heating, Z, from which P_1, the vapor pressure of monomer over that solution, can be obtained from the Clausius–Clapeyron equation and the Flory–Huggins equation. Thus

$$P_1 = \exp\left(\frac{-\Delta H_v}{RT} + i\right)\theta_1\ \exp[(1 - \theta_1) + \chi(1 - \theta_1)^2]. \quad (13)$$

If this pressure rises above ambient, boiling was considered to have occurred, and a lower heating

Table I Fixed Parameters Used in the Computation (See Ref. 10)

Symbol	Variable	Value	Units
$(C_1)_1$	WLF parameter for monomer	16.19	—
$(C_2)_1$	WLF parameter for monomer	13.27	K
$(C_1)_2$	WLF parameter for polymer	13.7	—
$(C_2)_2$	WLF parameter for polymer	49.3	K
K_{11}/ω	Free volume parameter for monomer	1.756×10^{-6}	$m^3\ kg^{-1}\ K^{-1}$
K_{12}/ω	Free volume parameter for polymer	5.127×10^{-7}	$m^3\ kg^{-1}\ K^{-1}$
$(T_g)_1$	Glass transition temperature for monomer	120	K
$(T_g)_2$	Glass transition temperature for polymer	442	K
$V_1(0)$	Monomer specific volume at 0 K	8.686×10^{-4}	$m^3\ kg^{-1}$
$V_2(0)$	Polymer specific volume at 0 K	7.975×10^{-4}	$m^3\ kg^{-1}$
ξ	Overlap factor	0.54	—
χ	Flory–Huggins interaction parameter	0.361	—

WLF, Williams–Landel–Ferry.

rate was tested until a critical rate, designed Z_c, was found that allows the polymer to degrade while keeping P_1 less than ambient throughout.

NUMERICAL ANALYSIS

The computer program searches for the critical heating rate, Z_c, at which the peak vapor pressure at the center of the cylinder, throughout the heating schedule, stays just below the ambient pressure. The critical rate, Z_c, was sought for various combinations of the parameters D_0, E_D, K_0, E, ΔH_v, and i that are, in principle, amenable to some degree of control when considering the intelligent design of copolymers.

In all computations, a cylinder of radius $r_0 = 2.5$ mm was considered, and the volume fraction of the inert filler, V_c, was taken to be 0.5. The values of all other constants and parameter values occurring in the model equations in the previous section are given in Table I.

Table II contains the five discrete values assigned at some stage of the computation to the six parameters: D_0, E_D, K_0, E, ΔH_v, and i. The center column gives the data used by Evans and colleagues[10] that corresponds to the model system poly(α-methylstyrene), which has been used to test the model experimentally. Temperature was varied in the range $393\ K \leq T \leq 1273K$, and data were considered unrealistic when $h(T = 393K) < 0.99$, because it implies that the polymer decomposes at temperatures below 393 K. Computations were truncated if $Z_c < 0.01\ K\ h^{-1}$ (in which case Z_c was taken as $0\ K\ h^{-1}$) or if $Z_c > 1000\ K\ h^{-1}$ (in which case Z_c was plotted as $1000\ K\ h^{-1}$).

The critical heating rates were calculated as functions of the pairs (E_D, D_o), $(\Delta H_v, i)$, and (K_o, E). For all pairs, each one of the four remaining parameters assumed, in turn, its five values given in Table II, whereas the other three remained fixed at the α-methylstyrene default values given in the center column of Table II. Clearly, for each of the three pairs, there are four sets of five profiles.

RESULTS AND DISCUSSION

The parameters selected for combined analysis are those that emerged as having the greatest

Table II Ranges for the Variable Parameters (Center Column Gives the Default Values)

Variable	Values					Units
D_o	6.92×10^{-5}	3.46×10^{-4}	6.92×10^{-4}	3.46×10^{-3}	6.92×10^{-3}	$m^2\ s^{-1}$
E_D	28.37×10^3	33.37×10^3	38.37×10^3	43.37×10^3	48.37×10^3	$J\ mol^{-1}$
K_o	1.67×10^{15}	8.35×10^{15}	1.67×10^{16}	8.35×10^{16}	1.67×10^{17}	s^{-1}
E	122×10^3	172×10^3	222×10^3	272×10^3	322×10^3	$J\ mol^{-1}$
ΔH_v	18.94×10^3	28.94×10^3	38.94×10^3	48.94×10^3	58.94×10^3	$J\ mol^{-1}$
i	21.255	21.755	22.255	22.755	23.255	ln (Pa)

influence on the critical heating rate when varied individually within the range of values that they could reasonably expect to take based on common polymers.[16] In that analysis, the remaining parameters were held at their default value, so the result conceals their combined effects on Z_c. The problem with such analyses lies not in their execution, but in the interpretation of results. Thus, it is possible to discover that a combination of very high ΔH_v and high D_o gives rise to values of Z_c, which are well in excess of 1000 K/h, but are unrealizable for the obvious reason that the high molecular weight of degradation product precludes a high value of D_0.

The commanding parameters so selected fall neatly into three groups. First are those that influence the transport properties, namely pre-exponential coefficient for diffusion, D_0, and activation energy for diffusion E_d [eq. (8)]. The latter influences the temperature dependence of diffusion; a low activation energy means that the diffusion coefficient is relatively high in the low temperature region. Second, there are those that control the temperature range over which thermal degradation occurs, namely the specific rate constant K_o and the activation energy for thermal degradation, E. The final pair of parameters influences the relationship between monomer concentration and boiling point, namely ΔH_v and i, the pre-exponential coefficient in the Clausius–Clapeyron equation.

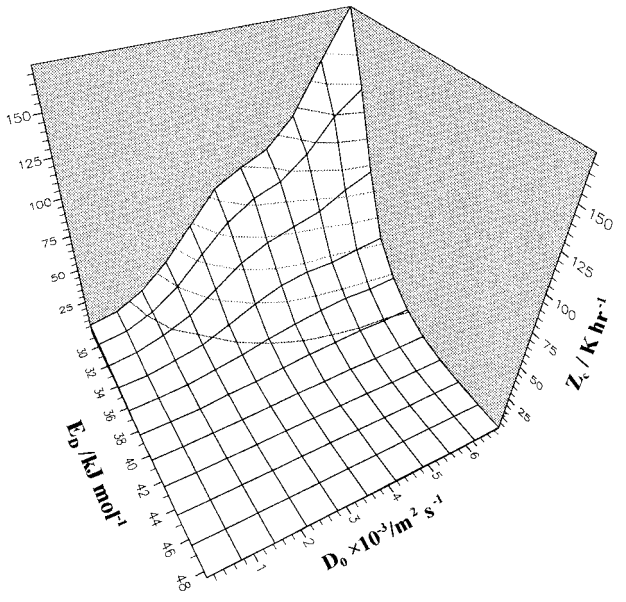

Peak Z_c at $D_0 = 7\times10^{-3}$m^{2}s^{-1}, E_D = 34 kJ mol^{-1}

K_0 / s^{-1}	Z_c /Khr^{-1}
1.67×10^{17}	175
8.35×10^{16}	212
1.67×10^{16}	325
8.35×10^{15}	390
1.67×10^{15}	550

Figure 2 Effect of systematic variations of K_0 (specific rate constant for thermal degradation) on Z_c for a basal plane representing transport properties (E_D– D_o).

Effect of Transport Properties

In the initial part of the study, the pre-exponential diffusion coefficient D_0 was varied with the activation energy for diffusion E_D over a range of values of the specific rate constant K_0. Thus, a series of five surfaces were obtained from plots of Z_c (vertical axis) against E_D and D_o (horizontal axes). Only one such surface is shown in Figure 2, because all surfaces had the same form but different heights. The surfaces show that Z_c is vanishingly small at low values of D_o and at high values of activation energy for diffusion. Conversely, Z_c rises to over 500 K h^{-1} at low activation energies and high D_o. Clearly, such high predicted heating rates, if realizable in practice, would invalidate the assumption that transient heating can be neglected.

The need for high D_o is transparent from these results, but low E_D arises because the diffusion coefficient must be reasonably high at low temperatures when thermal degradation is beginning to take place. This result captures the essence of the competition between the rate of generation of monomer and its transport to the free surfaces; both processes are crucially dependent on temperature, although activated by different mechanisms.

Figure 2 also lists the peak value of Z_c as a function of K_0, the specific rate constant for the thermal degradation reaction. As K_0 decreases, the corresponding thermogravimetric loss curve shifts to higher temperatures. Thus, the rate of monomer generation peaks at a high temperature, at which the effective diffusant coefficient, itself temperature-dependent, is greater. Thus, a picture, as yet blurred, begins to emerge to show how organic polymers might be deliberately synthesized to make this difficult stage in ceramic processing a rapid and facile step.

The next series of surfaces were generated with the same axes, but for systematic variation of the activation energy for thermal degradation, E. When this activation energy was low (E = 122 kJ mol^{-1}), Z_c was effectively zero for that part of the E_D–D_0 basal plane that was studied.

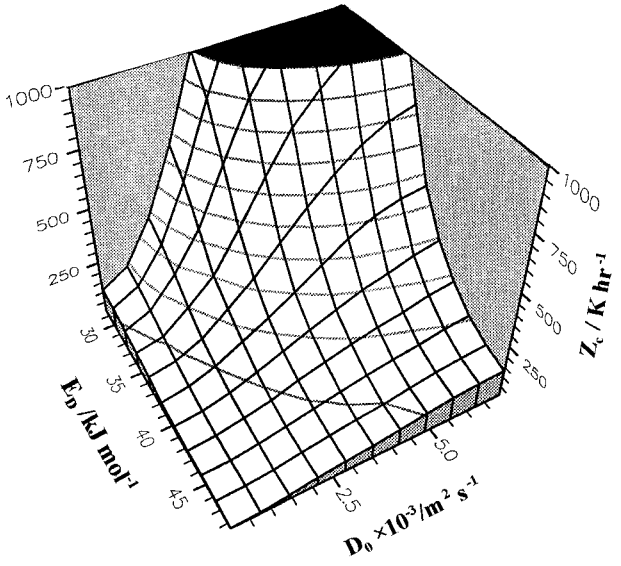

Peak Z_c at $D_0 = 7 \times 10^{-3} m^2 s^{-1}$, $E_D = 34$ kJ mol^{-1}

E/ kJmol^{-1}	Z_c/Khr^{-1}
172	61
222	325
272	875
322	>1000

Figure 3 Effect of systematic variations of E (activation energy for thermal degradation) on Z_c for a basal plane representing transport properties (E_D–D_o).

In fact, for this value of E, and for all the values of K_0 studied, degradation takes place below 100°C. A low activation energy for degradation means that substantial amounts of monomer are being generated in the low temperature regime where the transport to the surface is very slow. Because the monomer so generated cannot escape, the concentration rises very quickly to a high value at the center of the cylinder and boiling ensues. Conversely, when the activation energy for thermal degradation was high (Fig. 3), there was a substantial region over which Z_c was extremely high. A table is appended to Figure 3 showing the peak values of Z_c as a function of E, the form of the surfaces being similar in each case.

These two parts of the analysis show that the temperature range over which thermal degradation takes place must be matched to the temperature region over which the transport coefficient is high. Although this is an unsurprising result, it has never been taken into account in the selection, yet alone in the deliberate synthesis of polymers for this application. It clearly points to the selection of a polymer in which the backbone should have a high bond energy, and this in turn influences the nature of side groups that could be appended.

In the next computational experiment, the same horizontal axes representing the transport properties were used, and Z_c was plotted as ordinate for a range of values of enthalpy of vaporization ΔH_v. The enthalpy of vaporization emerges as the single strongest parameter in this study (as shown by Fig. 4). For $\Delta H_v = 19$ kJ mol^{-1}, all the Z_c values were < 1 K h^{-1} [Fig. 4(a)], but where $\Delta H = 59$ kJ mol^{-1} a substantial area of the

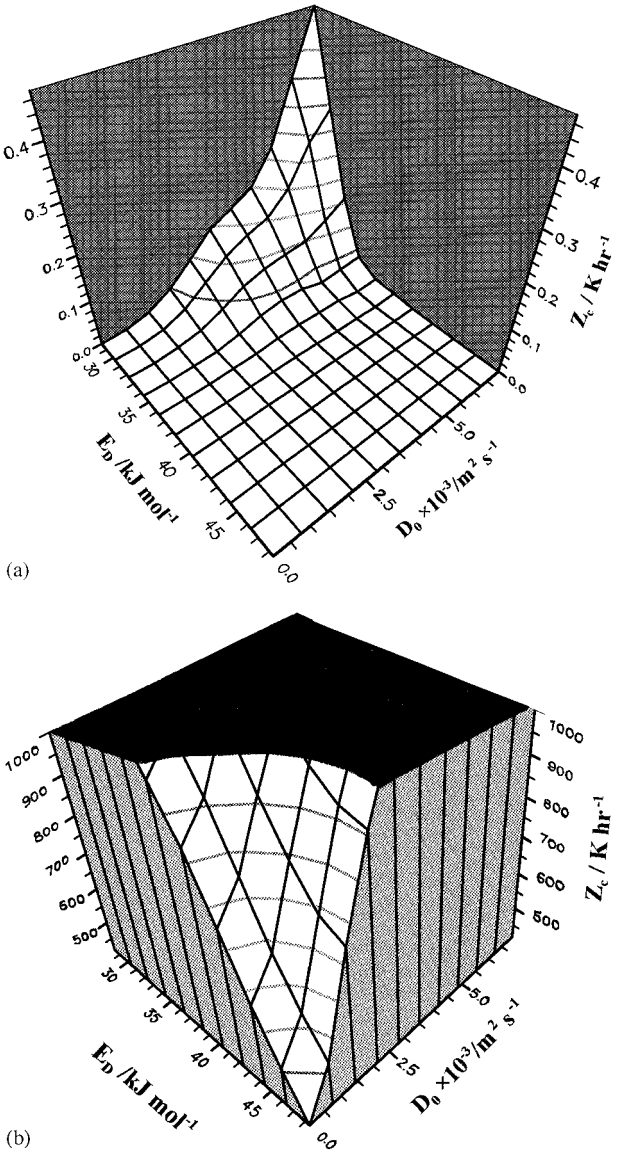

Figure 4 Remarkable effect of ΔH_v (enthalpy of vaporization of degradation product) on Z_c for the basal plane representing transport properties (E_D–D_o). (a) $\Delta H_v = 18.9$ kJ mol^{-1}; (b) $\Delta H_v = 58.8$ kJ mol^{-1}.

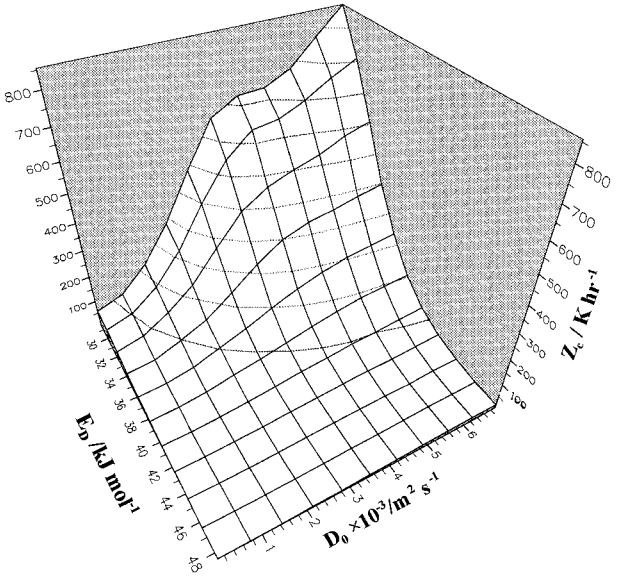

Peak Z_c at $D_0 = 7 \times 10^{-3} m^2 s^{-1}$, $E_D = 34$ kJ mol^{-1}

i / ln(Pa)	Z_c /Khr^{-1}
23.26	85
22.76	167
22.26	325
21.76	622
21.26	855

Figure 5 Effect of systematic variations of i on Z_c for a basal plane representing transport properties (E_D–D_o). Figure is for i = 22–26.

transport parameter space explored presents $Z_c > 800$ K h^{-1} [Fig. 4(b)]. As discussed previously, such high values of Z_c violate the assumption that transient heating can be neglected, but this does not deny the prediction of very high values of Z_c.

Equation (13) shows that, as ΔH_v is increased, the vapor pressure is reduced. Conversely, as the pre-exponential coefficient i is increased, the vapor pressure is increased. Figure 5 shows that the lowest value of i = 21.26 studied gives a peak Z_c of just over 800 K h^{-1}. Its effect is somewhat less strong than that of ΔH_v. Of course, there are other parameters that affect the vapor pressure over solution, principally the Florry–Huggins interaction parameter; but, in previous work,[16] they were found to be less influential.

Clearly, the vapor pressure of the degradation product over solution is influenced both by degree of polarity and molecular weight. Thus, a copolymer can be envisaged in which, at intervals, the backbone is weakened either by a conjugated carbon—carbon bond or by the attachment of a side group with high electron affinity. The distance between such groups would determine the fragment size and hence ΔH_v.

Effect of Vapor Pressure Parameters

When the parameter space corresponding to the variables that influence vapor pressure was explored, the surfaces generated all showed the steepest gradients, as expected from the overriding influence of ΔH_v. Thus, the region of the basal plane corresponding to a high value of i and a low value of ΔH_v consistently gave a negligibly small value of Z_c. At low values of D_o, Z_c was also low at the end of the plane corresponding to a high value of i [Fig. 6(a)], but when a high value of D_o was tested, a high Z_c could be obtained parallel to the i axis [Fig. 6(b)].

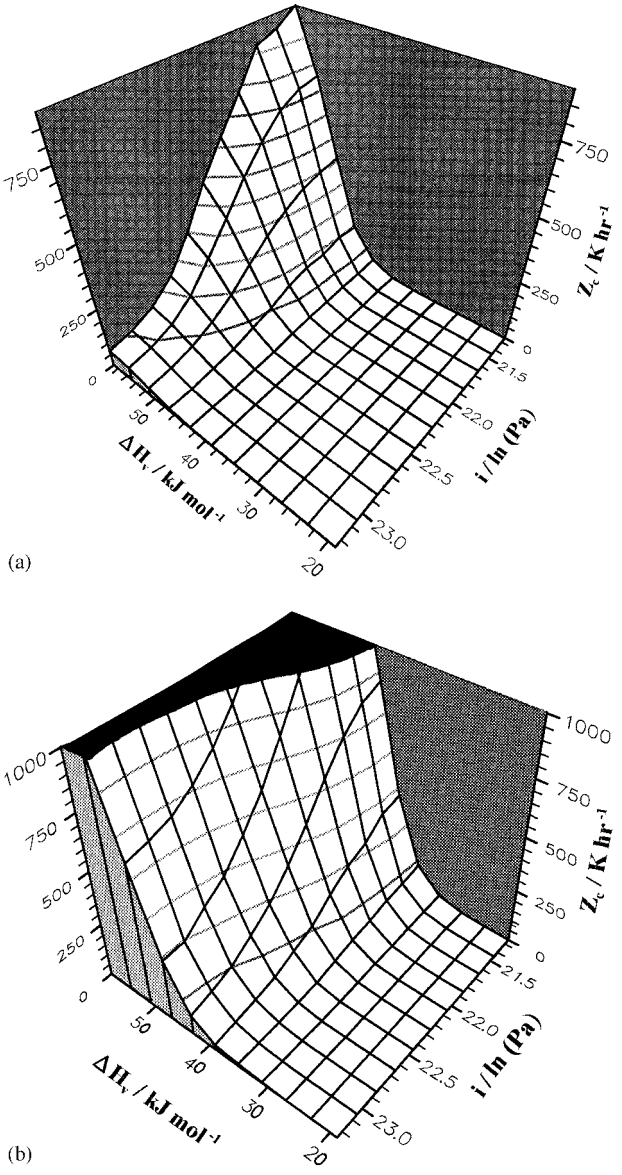

Figure 6 Effect of variations in D_o on Z_c for the basal plane representing boiling of monomer (ΔH_v–i). (a) $D_o = 6.9 \times 10^{-5}$ m^2 s^{-1}. (b) $D_o = 8.9 \times 10^{-3}$ m^2 s^{-1}.

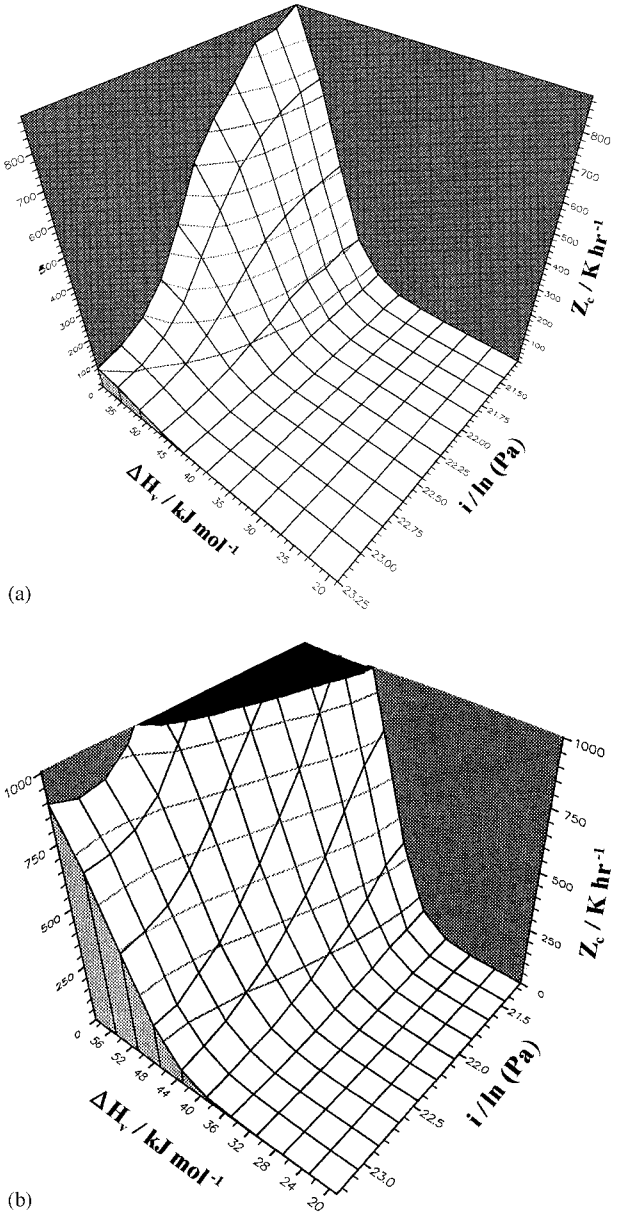

Figure 7 Effect of variation in activation energy for diffusion E_D, on Z_c for the basal plane representing boiling of monomer (ΔH_v–i). (a) E_D = 48.4 kJ mol^{-1}; (b) E_D = 28.4 kJ mol^{-1}.

Very similar behavior was obtained when the activation energy for diffusion was taken as the third variable. At high values of E_D [Fig. 7(a)], the surface was very similar to that in Fig. 6(a). High activation energy for diffusion results in a low coefficient of diffusion at low temperatures. Low vapor pressure can nevertheless compensate for this. At high values of E_D, the influence of i is removed and Figure 7(b) is very similar to Figure 6(b).

The value of K_0, the specific rate constant for thermal degradation, had only a limited effect on the surfaces. A representative surface corresponding to $K_0 = 1.67 \times 10^{16}$ s^{-1} (the midpoint) is shown in Figure 8. The other surfaces differed mainly in the intercept at i = 23.25, ΔH_v = 60 kJ mol^{-1}, which is tabulated in Figure 8.

In contrast, varying E, the activation energy, for thermal degradation on the vapor pressure basal plane had a dramatic effect on the surfaces. At E = 122 kJ mol^{-1}, the computer program gives unrealistic values because of degradation below 100°C. At E = 172 kJ mol^{-1} [Fig. 9(a)], about half the basal plane corresponded to Z_c values that were negligibly small. Where E = 322 kJ mol^{-1}, only the high ΔH_v–low i region of the basal plane offered high Z_c [Fig. 9(b)].

Effect of Decomposition Parameters

Finally, the parameters that influence the thermogravimetric curve, K_0 and E, were plotted as the basal plane. Figure 10 shows the effect of

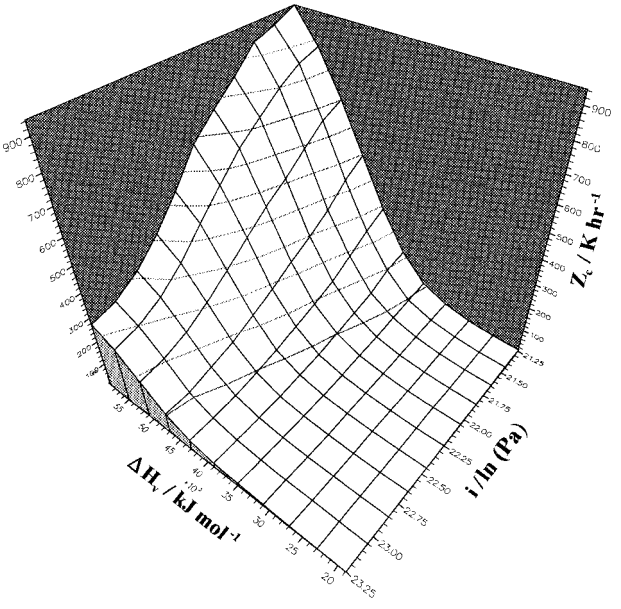

Peak Z_c at i =23.25 ln (Pa), ΔH_v =60 kJmol^{-1}

K_0 / s^{-1}	Z_c /Khr^{-1}
1.67×10^{15}	260
8.35×10^{15}	305
1.67×10^{16}	350
8.35×10^{16}	490
1.67×10^{17}	585

Figure 8 Effect of systematic variations in the specific rate constant for thermal degradation K_0 on Z_c for the basal plane representing boiling of monomer (ΔH_v–i). Figure is for $K_0 = 1.67 \times 10^{15}$ s^{-1}.

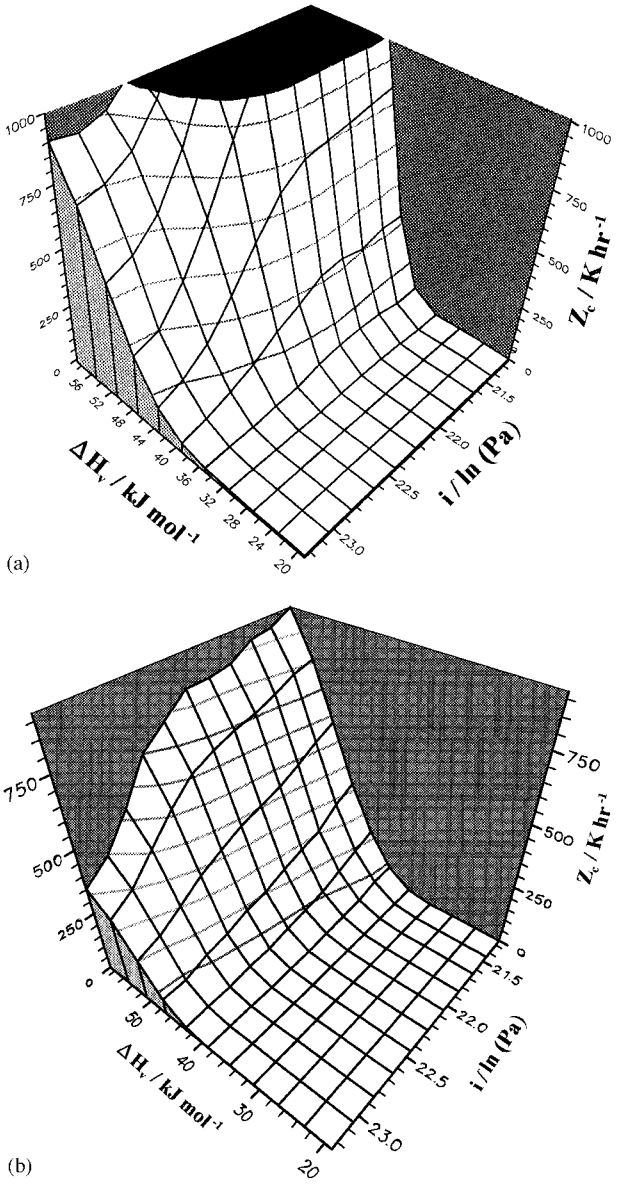

Figure 9 Effect of activation energy for thermal degradation on Z_c for the basal plane representing boiling of monomer (ΔH_v–i). (a) $E = 172$ kJ mol^{-1}; (b) $E = 322$ kJ mol^{-1}.

varying D_o on the critical heating rate. At low D_o [Fig. 10(a)], values of Z_c are low throughout the basal plane. At high D_o [Fig. 10(b)], a ridge of high Z_c corresponds to a high activation energy for thermal degradation (decomposition and liberation of products at high temperatures), and the effect of K_0 is secondary.

This behavior is also seen when E_D is varied systematically (Fig. 11). A combination of low E_D and high E consistently gives high critical heating rate. The high E means that decomposition occurs in the high temperature regime, and low E_D means that the diffusion coefficient is high over a wide temperature range.

Predictably, when the value of Z_c on this basal plane is explored for different values of ΔH_v, the effect is dramatic. Figure 12(a) shows the effect of low ΔH_v (a degradation product with a low boiling point) that gives very low values of Z_c throughout the plane. When ΔH_v is high [Fig. 12(b)], high Z_c is achieved across the basal plane, except for $E = 122$ kJ mol^{-1}, where the combination of E and K_o gives a thermogravimetric curve for which degradation is complete below 100°C. This is unlikely to represent a real system, and the model does not accommodate diffusion calculated below 100°C, because diffusion is so low that Z_c is zero. The effect of i is similar to that of ΔH_v, but less pronounced; a high i corresponds to low Z_c.

CONSEQUENCES FOR MATERIALS SELECTION AND SYNTHESIS

In principle, the analysis presented herein provides a foundation for the deliberate synthesis of polymers that will enable a ceramic body to survive the critical initial stage of thermolysis without disrupting the assembly of particles. At a later stage, continuous porosity develops and gas transport assists the displacement of organic matter. In practice, the realization of this goal is complicated because the ranges of values for the six parameters studied place conflicting demands on bonding and on structure.

In many ways, the simplest variable to address is the enthalpy of vaporization of the degradation product. There have been many attempts to relate ΔH_v to other parameters.[20–22] The enthalpy itself depends on temperature, and Yaws and Yang[20] have correlated ΔH_v at a temperature T to ΔH_v^1 at the normal boiling point T_1 and to the critical temperature T_c by

$$\Delta H_v = \Delta H_v^1 \left(\frac{T_c - T}{T_c - T_1} \right)^{0.38} \tag{14}$$

for 700 organic liquids. Perhaps one of the most useful surveys for this purpose is by Nikolaev and coworkers,[21] in which ΔH_v is given by

$$\Delta H_v = f\left[I \frac{m}{d} \frac{(n^2 - 1)}{(n^2 - 2)} \right] \tag{15}$$

where I is the ionization potential, m is the molecular weight, d is the density, and n is the

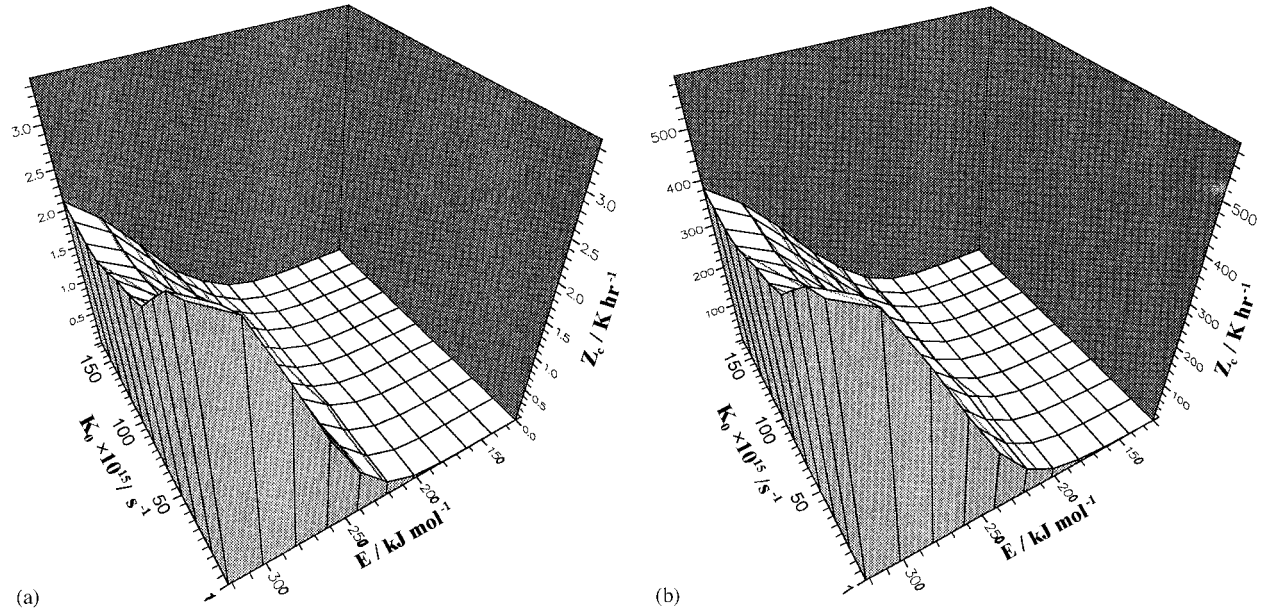

Peak Z_c at $K_0 = 1.67 \times 10^{15}$ s^{-1}, E = 322 kJmol^{-1}

D_0 /m^{2}s^{-1}	Z_c /Khr^{-1}
6.92×10^{-5}	4
3.46×10^{-4}	25
6.92×10^{-4}	54
3.46×10^{-3}	321
6.92×10^{-3}	692

Figure 10 Effect of D_o on Z_c for the basal plane representing thermal degradation (K_o– E). (a) $D_o = 6.92 \times 10^{-5}$ m^2 s^{-1}. (b) $D_o = 6.92 \times 10^{-3}$ m^2 s^{-1}.

refractive index. When ΔH_v is plotted against the function on the rhs of eq.(15) for a selection of aromatic and aliphatic hydrocarbons, it gives an average slope of 2.8×10^{27} m^{-3} and intercept at $\Delta H_v = RT$ (2.48 kJ mol^{-1} at 298 K). There is a slight spread in the results that corresponds to a lower slope for aromatic or cyclic hydrocarbons, compared with that for aliphatics. A comparable plot for polar liquids gives slopes of 4.6×10^{27} m^{-3} and 3.0×10^{27} m^{-3} for aliphatic and aromatic compounds, respectively.

Thus, for the same value of the function of molecular weight, density, refractive index, and ionization potential given in eq. (15), the enthalpy of vaporization follows the following trend: aromatic and cyclic hydrocarbons < aliphatic hydrocarbons < polar aromatics < polar aliphatics. Ionization energies for a wide range of organic molecules are tabulated.[23] The effect of molecular weight is shown by a range of expressions for vapor pressure[24] and provides the main route to control of ΔH_v through fragment size.

Thus, the degradation product molecular weight could, in principle, be controlled by the judicious selection of carbon—carbon bonds in the backbone interspersed with weak units or with bonds weakened by side groups with high electron affinity placed at intervals.

Activation energy for thermal degradation E is clearly related to bond energy, and the predicted desire for high E may conflict with a deliberately weakened chain at selected sites. The literature gives very few values of K_0, but clearly a low value of K_0 corresponds to a high stability polymer. This is achieved in engineering polymers through the use of recurring aromatic groups and ether linkages, but a complicating factor in ceramic processing is that the polymer should decompose to leave no carbon residue.

A more serious problem surrounds the acquisition of key transport data D_o and E_D that appear in eq. (8), as well as the ratio of solvent and polymer jumping units. A limited number of systems have been analyzed using this free volume theory and, for those that have, available data are tabulated in Table III. In later assessments of the Vrentas–Duda theory,[25,26] the activation energy for diffusion E_D is considered to be concentration-

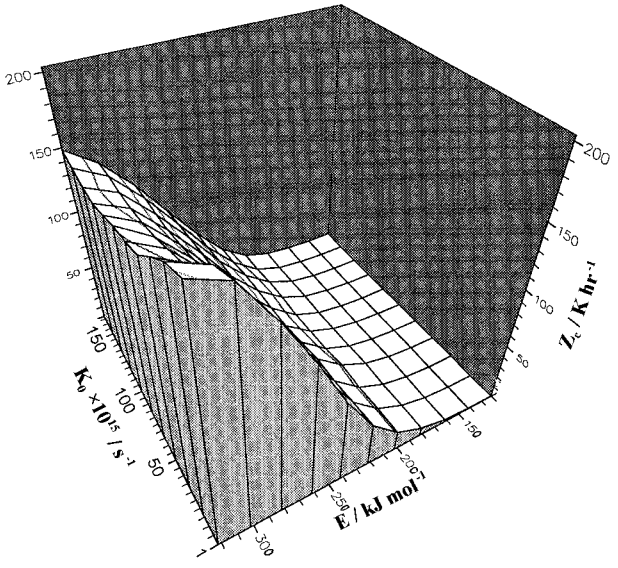

Peak Z_c at $K_0 = 1.67 \times 10^{15}$ s^{-1}, E = 322 kJmol^{-1}

E_D / kJmol^{-1}	Z_c /Khr^{-1}
28.37	226
33.37	111
38.37	54
43.37	25
48.37	11

Figure 11 Effect of activation energy for diffusion E_D on Z_c for the basal plane representing thermal degradation (K_0–E), $E_D = 28.4$ kJ mol^{-1}.

dependent, and estimates of the remaining parameters D_o and ξ are based on the assumption $E_D = 0$ at all concentrations. This does, however, contribute to the deviation of predictions from experimental data.[25]

D_o is considered to be a solvent-dominated parameter, and this is confirmed by experimental measurements in which D_o emerges as identical for the same diffusant in different polymers. Treating it as a solvent property opens the door to the estimation of all the parameters in the free volume equation without reference to solvent polymer diffusion data.[25]

CONCLUSIONS

This exploration of the combined effects of the three sets of parameters that influence the formation of defects in the thermolysis of ceramic moldings provides a set of criteria for intelligent polymer synthesis. Consistently high critical rates are obtained for a low activation energy for diffusion and a high pre-exponential D_o. Values of parameters controlling polymer decomposition are preferred if they produce onset of decomposition at a high temperature, corresponding to the tempera-

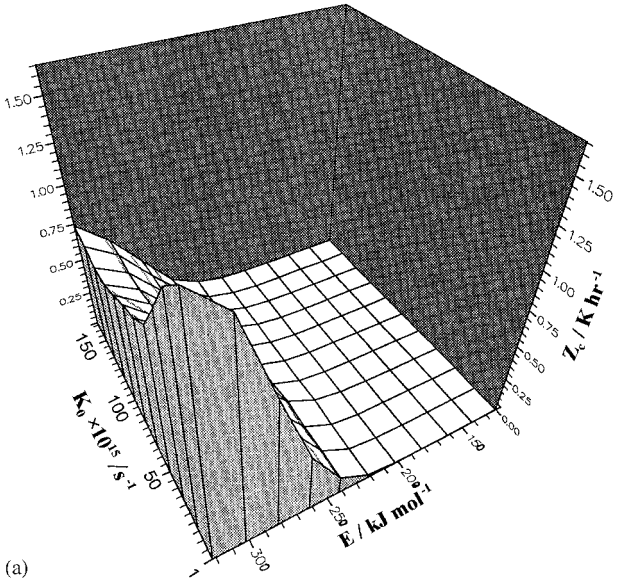

(a)

Peak Z_c at $K_0 = 1.67 \times 10^{15}$ s^{-1}, E = 322 kJmol^{-1}

ΔH_v / kJmol^{-1}	Z_c /Khr^{-1}
19	2
29	11
39	54
49	227
59	882

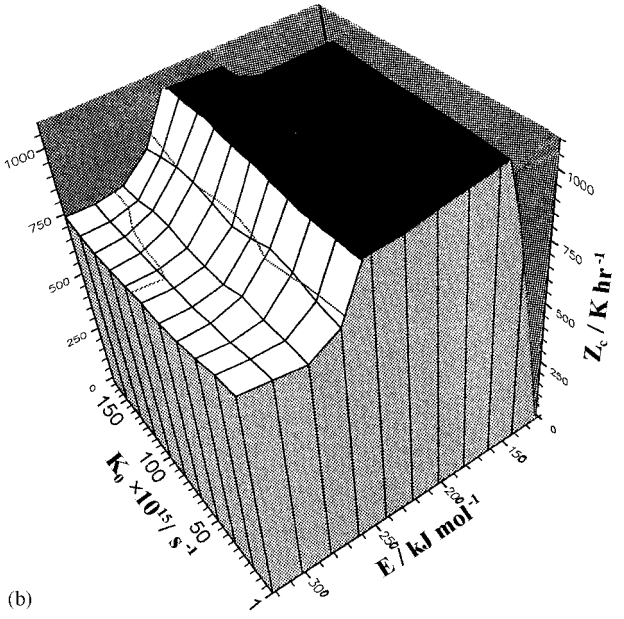

(b)

Figure 12 Effect of ΔH_v on Z_c for the basal plane representing thermal degradation (K_0–E). (a) $\Delta H_v = 18.9$ kJ mol^{-1}; (b) $\Delta H_v = 58.9$ kJ mol^{-1}.

Table III Values of Diffusion Parameters for Polymer-Solvent Systems

Polymer	Solvent	D_o (m^2 s^{-1})	ξ	E_D (kJ mol^{-1})	Source
Polystyrene	Toluene	6.15×10^{-6}	0.53	22	17
Poly(methylacrylate)	Methyl acetate	8.71×10^{-6}	0.57	15	17
Polystyrene	Ethylbenzene	6.92×10^{-6}	0.56	38	17
Polystyrene	Toluene	4.82×10^{-6}	0.58	0	25
Poly(vinyl acetate)	Toluene	4.82×10^{-6}	0.82	0	25
Polystyrene	Ethylbenzene	4.61×10^{-6}	0.69	0	25

ture region under which mass transport rates are high. The enthalpy of vaporization emerges as an overridingly influential variable in all the calculations performed, often able to compensate for unfavorable values of other parameters.

The authors thank Mrs. K. Goddard for typing the manuscript.

NOMENCLATURE

C	concentration of monomer in solution in the polymer phase based on the total volume of suspension	kg m^{-3}
D	diffusion coefficient in polymer	m^2 s^{-1}
D_c	diffusion coefficient in suspension	m^2 s^{-1}
D_o	pre-exponential factor in eq. (8)	m^2 s^{-1}
d	density	kg m^{-3}
E_D	activation energy for diffusion	J mol^{-1}
E	activation energy for thermal degradation	J mol^{-1}
ΔH_v	enthalpy of vaporization	J mol^{-1}
ΔH_v^1	enthalpy of vaporization at the boiling point	J mol^{-1}
h	fraction of mass of polymer remaining	$0 < h < 1$
I	ionization potential	J
i	constant in eq. (13)	ln (Pa)
K_{11}	free volume parameter for monomer	m^3 kg^{-1} K^{-1}
K_{12}	free volume parameter for polymer	m^3 kg^{-1} K^{-1}
m	molecular weight	kg m L^{-1}
n	refractive index	—
P_1	vapor pressure of monomer over solution	Pa
$\dot{q}$	rate of production of monomer based on mass of polymer	s^{-1}
$\dot{Q}$	rate of production of monomer based on total volume of suspension	kg m^{-3} s^{-1}
R	gas constant	J mol^{-1} K^{-1}
r	radius	m
r_0	radius of cylindrical molding	m
r_n	radius of the polymer-containing core	m
T	temperature	K
T_1	boiling point	K
T_c	critical temperature	K
$(T_g)_1$	glass transition temperature of monomer	K
$(T_g)_2$	glass transition temperature of polymer	K
V_f	average hole-free volume per unit mass	m^3 kg^{-1}
$V_1(0)$	specific volume of monomer at 0 K	m^3 kg^{-1}
$V_2(0)$	specific volume of polymer at 0 K	m^3 kg^{-1}
V_c	powder volume loading	$0 < V_c < 1$
W_1	weight fraction of polymer in polymer-monomer solution	$0 < W_1 < 1$
W_2	weight fraction of polymer in polymer-monomer solution	$0 < W_2 < 1$
Z	heating rate	K s^{-1}
Z_c	critical heating rate	K s^{-1}
ϕ	volume fraction of monomer in polymer	$0 < \phi < 1$
χ	interaction parameter for polymer-monomer system	—
ω	overlap factor for free volume	—

REFERENCES

1. M. J. Edirisinghe and J. R. G. Evans, *Int. J. High Tech. Ceram.,* **2,** 1 and 249 (1986).
2. B. C. Mutsuddy and R. G. Ford, *Ceramic Injection Moulding,* Chapman & Hall, London, 1995.
3. J. R. G. Evans, in *Processing of Ceramics. Part I. Materials Science and Technology Series,* Vol. 17A, R. J. Brook, Ed., VCH Weinheim, Germany, 1996, Chap. 8.
4. A. Johnsson, E. Carlstrom, L. Hermansson, and R. Carlsson, *Proc. Br. Ceram. Soc.,* **33,** 139 (1983).
5. K. Saito, T. Tanaka, and T. Hibino, UK Pat. 1,426,317, February 25, 1976.
6. S. J. Stedman and J. R. G. Evans, *Ceram. Int.,* **16,** 107 (1990).
7. J. K. Wright, J. R. G. Evans, and M. J. Edirisinghe, *J. Am. Ceram. Soc.,* **72,** 1822 (1989).
8. J. K. Wright and J. R. G. Evans, *J. Mater. Sci.,* **26,** 4897 (1991).
9. P. Calvert and M. Cima, *J. Am. Ceram. Soc.,* **73,** 575 (1990).
10. J. R. G. Evans, M. J. Edirisinghe, J. K. Wright, and J. Crank, *Proc. Roy. Soc. Lond.,* **A432,** 321 (1991).
11. H. M. Shaw and M. J. Edirisinghe, *Phil. Mag. A,* **A72,** 267 (1995).
12. S. A. Matar, M. J. Edirisinghe, J. R. G. Evans, and E. H. Twizell, *J. Am. Ceram. Soc.,* **79,** 749 (1996).
13. J. H. Song, M. J. Edirisinghe, J. R. G. Evans, and E. H. Twizell, *J. Mater. Res.,* **11,** 830 (1996).
14. J. H. Song, J. R. G. Evans, M. J. Edirisinghe, and E. H. Twizell, *A.I.Ch.E.J.,* **42,** 1715 (1996).
15. P. D. Hammond and J. R. G. Evans, *Chem. Eng. Sci.,* **50,** 3187 (1995).
16. S. A. Matar, J. R. G. Evans, M. J. Edirisinghe, and E. H. Twizell, *J. Mater. Res.,* **10,** 2060 (1995).
17. J. L. Duda, J. S. Vrentas, S. T. Ju, and H. T. Liu, *A.I.Ch.E.J.,* **28,** 279 (1982).
18. R. M. Barrer, in *Diffusion in Polymers,* J. Crank and G. S. Park, Eds., Academic Press, London, 1968, p. 165.
19. S. A. Matar, M. J. Edirisinghe, J. R. G. Evans, E. H. Twizell, and J. H. Song, *J. Mater. Sci.,* **30,** 3805 (1995).
20. L. L. Yaws and H. C. Yang, *Hydrocarbon Proc.,* **69,** 87 (1990).
21. V. F. Nikolaev, A. N. Vereshchagin, and S. I. Strobykin, *Bull. Acad. Sci. USSR. Div. Chem.,* **38,** 2609 (1989).
22. S. F. Abdulnur, *J. Am. Chem. Soc.,* **98,** 4039 (1976).
23. V. I. Vedeneyev, L. V. Gurvich, V. N. Kondratyev, V. A. Medvedev, and Y. L. Frankevich, *Bond Energies, Ionization Potentials and Electron Affinities,* Arnold, London, 1966.
24. J. R. Partington, *An Advanced Treatise on Physical Chemistry,* Vol. 2, Longmans, London, 1968, p. 226.
25. J. M. Zielinski and J. L. Duda, *A.I.Ch.E.J.,* **38,** 405 (1992).
26. J. M. Zielinski and J. L. Duda, in *Polymer Devolatilization,* R. J. Albalak, Ed., Marcel Dekker, New York, 1996, p. 35.